Central European Journal of Energetic Materials
ISSN 1733-7178; e-ISSN 2353-1843

Cent. Eur. J. Energ. Mater. 2017, *14*(2): 281-295 DOI: 10.22211/cejem/69299

A Facile Synthesis of 3,3'-Dinitro-5,5'-diamino-bi-1,2,4-triazole and a Study of Its Thermal Decomposition

Qing Ma,* Huanchang Lu, Yanyang Qu, Longyu Liao, Jinshan Li, Guijuan Fan, Ya Chen

Institute of Chemical Materials, China Academy of Engineering Physics, Mailbox 311-919, Mianyang, Sichuan, 621900 Mianyang, China
**E-mail: maq@caep.cn*

Abstract: 3,3'-Dinitro-5,5'-diamino-bi-1,2,4-triazole (DABNT) was synthesized by a facile method and its crystalline density was determined as 1.839 g·cm^{-3} at 293(2) K by X-ray diffraction. Its thermal decomposition kinetics and mechanism were studied by means of differential scanning calorimetry-thermogravimetry (DCS-TG), *in situ* thermolysis by rapid-scan Fourier transform infrared spectroscopy (RSFTIR) and simultaneous TG-IR technology. The results showed that the apparent activation energies obtained by the Kissinger, Ozawa and Starink methods were 122.9 kJ·mol^{-1}, 123.2 kJ·mol^{-1} and 123.5 kJ·mol^{-1}, respectively. The thermodynamic parameters of $\Delta S^{\neq}$, $\Delta H^{\neq}$ and $\Delta G^{\neq}$ were −37.5 J·K^{-1}·mol^{-1}, 118.4 kJ·mol^{-1} and 138.7 kJ·mol^{-1}, respectively. The decomposition reaction process of DABNT starts with the transformation from a primary amine to a secondary amine and then the loss of one nitro-group from the DABNT structure. Gaseous products, such as N_2O and H_2O, were detected from decomposition in the range of 50-300 °C. Density functional theory (DFT) calculations were further employed to illustrate the decomposition mechanism. The above-mentioned information on the synthesis and thermal behaviour is quite useful for the scale-up and evaluation of the thermal safety of DABNT.

Keywords: 3,3'-dinitro-5,5'-diamino-bi-1,2,4-triazole, facile synthesis, DSC-TG, RSFTIR, TG-IR, thermolysis

1 Introduction

Poly-nitro-azole compounds are a series of attractive energetic materials, which usually possess positive heats of formation, good thermal stability, acceptable

sensitivity, and great detonation performance owing to the N−N, N=N and C−N bonds [1, 2]. However, the NH moieties of imidazole [3-5], pyrazole [6,7], carbazole [8,9], triazole [10, 11], and tetrazole [12] could cause acidity and hygroscopicity for azole-based energetic materials. To the best of our knowledge, various methods have been considered for modifying the frameworks of azole-energetic materials, and for generating great anions in most cases, which apparently became a good solution to the acidity and hygroscopy issues [13-16]. In order to further increase the energy of energetic salts, nitramine azole compounds were recently synthesized based on the C−NH_2 or N−NH_2 groups [17-21] instead of just synthesizing salts *via* the NH moieties. Among the N-functionalizing methodologies, N-amination is one of the most attractive strategies for eliminating the acidity and enhancing the energy, which usually require the assistance of electrophilic aminating reagents such as monochloramine (NH_2Cl), hydroxylamine-O-sulfonic acid (HOSA), O-(2,4-dinitrophenyl)-hydroxylamine ($DnpONH_2$), O-mesitylenesulfonyl hydroxylamine (MSH) and O-tosylhydroxylamine (THA). With great progress in the development of N-aminating reagents, a series of N-amino azole-based energetic compounds were synthesized and most of them possessed low sensitivity and a comparatively high decomposition temperature due to the inter- and intra-molecular hydrogen-bonding interactions between the amino and nitro groups [22-26]. Recently, 3,3'-dinitro-5,5'-diamino-bi-1,2,4-triazole (DABNT) was reported by Chavez *et al*. [27] and by Shreeve *et al*. [28]. DABNT is considered as a potential replacement candidate for 1,3,5-trinitro-1,3,5-triazacyclohexane (RDX) since it has superior detonation performance ($D = 8.7$ km·s^{-1}, $P = 32$ GPa). Additionally, it is worth noting that its impact sensitivity (IS) is 78 J (corresponding to an h_{50} exceeding 318 cm when the drop hammer is 2.5 kg) and its friction sensitivity (FS) is 360 N, which indicates that the sensitivities of DABNT are basically equal to those of the traditional insensitive high-energy explosive (IHE) 1,3,5-triamino-2,4,6-trinitrobenzene (TATB) (h_{50} exceeds 320 cm when the drop hammer is 2.5 kg).

The scale-up for new explosives centres on atom-economy and environmentally-friendly synthetic methods [29], as well as their thermochemical properties [30]. Compared with previous methods, DABNT was prepared in this work by a facile synthesis, without separation of intermediates or chromatography (Scheme 1), which is suitable for the scale-up. Subsequently, the non-isothermal kinetic performance and decomposition behaviour were also investigated in detail.

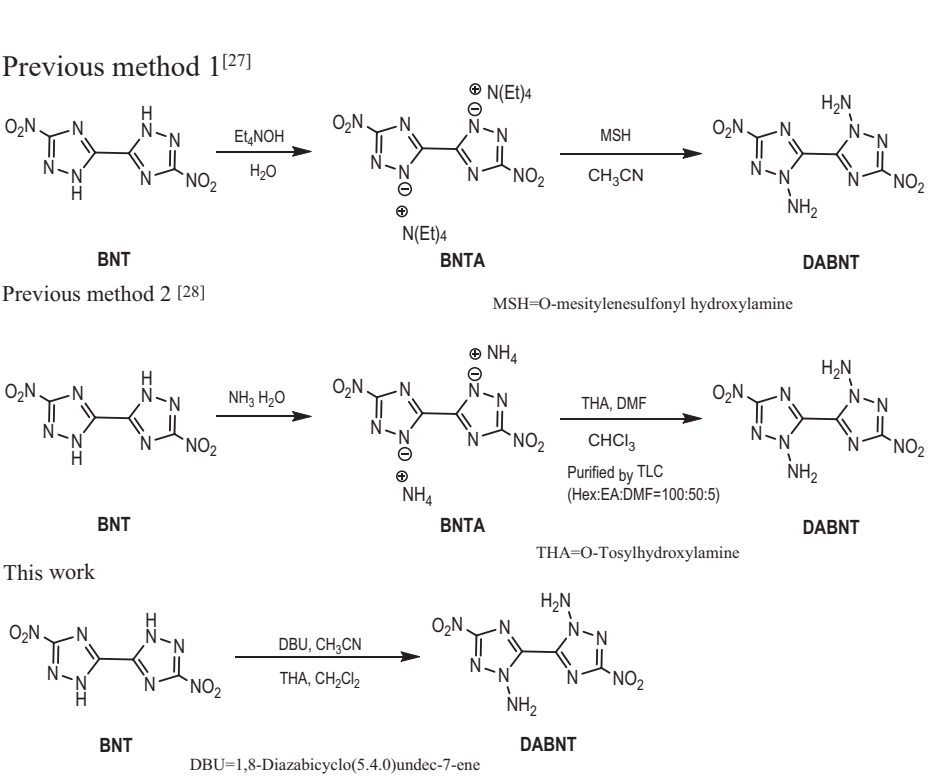

Scheme 1. The synthetic paths for DABNT

2 Experimental

2.1 Materials and instruments

All chemicals used in this research were analytical grade materials purchased from Alfa Aesar or J & K without further purification. ^{1}H and ^{13}C NMR spectra were recorded on a Bruker 600 MHz nuclear magnetic resonance spectrometer operating at 600 MHz and 150 MHz, respectively, and referenced to Me_4Si. Elemental analyses (C, H, N) were carried out on an elemental analyzer (Vario EL Cube, Germany). Decomposition points (onset) were recorded on a differential scanning calorimeter-thermal gravimetric instrument (TGA/DSC1, METTLER TOLEDO LF/1100). The thermal stabilities of DABNT were determined by differential scanning calorimetry (DSC) and thermogravimetry (TGA) at heating rates of 5 $K \cdot min^{-1}$, 10 $K \cdot min^{-1}$, 15 $K \cdot min^{-1}$, and 20 $K \cdot min^{-1}$ in open aluminum pans. Infrared (IR) spectra were measured on a Thermofisher Nicolet 800 FT-IR spectrometer in the range of 4000-400 cm^{-1} as KBr pellets at 20 °C. High-

resolution mass spectrometry (ESI-HRMS) was carried out on a Shimadzu LCMS-IT-TOF mass spectrometer. Rapid scanning Fourier transform infrared spectroscopy (RSFTIR) was measured using a Thermofisher Nicolet 6700 FT-IR spectrophotometer and an *in situ* thermolysis cell in the temperature range of 50-300 °C and at a heating rate of 5 °C·min^{-1}. Thermogravimetry-infrared spectroscopy (TG-IR) was performed by employing a Netzsch TG 209 cell (Germany) and Bruker FTIR Vector 22 under nitrogen gas at 5 °C·min^{-1}.

2.2 Synthesis of 3,5-dinitro-2,2'-diamino-bi-1,2,4-triazole (DABNT)

3,3'-Dinitro-bi-1,2,4-triazole dihydrate (BNT·2H_2O) [10] and O-tosylhydroxylamine (THA) [31, 32] were synthesized according to literature methods.

3,5-Dinitro-2,2'-diamino-bi-1,2,4-triazole (DABNT): A mixture of BNT·2H_2O (2 mmol, 0.5 g) and 1,8-diazabicyclo[5,4,0]undec-7-ene (DBU) (4 mmol, 0.6 g) in acetonitrile (10 mL) was stirred at room temperature for 1 h. Freshly prepared THA (12.5 mmol, 1.4 g) in dichloromethane (30 mL) was added in one portion to this orange solution and the mixture was stirred for another 3 h. The precipitate was then filtered off and washed with acetonitrile (5 mL). The combined organic phases was concentrated and the final crude product was added to water (10 mL) with grinding to yield pure DABNT (as a white solid, 0.27 g, 56.4%). ^{1}H NMR (600 MHz, DMSO-d_6) $\delta = 7.52$ ppm; ^{13}C NMR (150 MHz, DMSO-d_6) $\delta = 158.30$, 140.91 ppm; elemental analysis (%, $C_4H_4N_{10}O_4$) calcd. C 18.7, H 1.5 N 54.6, found C 18.5, H 1.8, N 54.9; HRMS (ESI): *m/z* calcd. for $C_4H_4N_{10}O_4$: 255.0342; found 255.0339.

3 Results and Discussion

3.1 X-ray diffraction and morphology

A colourless block of $0.30 \times 0.25 \times 0.20$ mm for DABNT single-crystal analysis was mounted on a MicroMesh™ (MiTeGen) using a small amount of Cargille Immersion Oil. Data were collected on a Bruker three-circle platform diffractometer equipped with a SMART APEX II CCD detector. A Kryo-Flex low temperature device was used to keep the crystals at a constant 293(2) K during data collection. Data collection was performed and the unit cell was initially refined using APEX2. Data Reduction was performed using SAINT and XPREP. Corrections were applied for Lorentz, polarization, and absorption effects using SADABS. The structures were solved and refined with the aid of the programs using Direct Methods and least squares minimization by the SHELXS-97 and

SHELXL-97 programs [33, 34]. The full-matrix least-squares refinement on F^2 included atomic coordinates and anisotropic thermal parameters for all non-H atoms. The H atoms were included using a riding model. The non-hydrogen atoms were refined anisotropically. The hydrogen atoms were located and refined. Crystals of DABNT are shown in Figure 1, indicating that the crystal of DABNT is rectangular in shape.

Table 1. Crystallographic data and structure refinement of DABNT

Compound	DABNT
Empirical formula	$C_4H_4N_{10}O_4$
Formula weight [g·mol^{-1}]	256.17
Crystal system	Monoclinic
Space group	$P2_1/n$
Crystal size [mm]	0.30 × 0.25×0.20
a [Å]	8.0118(19)
b [Å]	13.042(3)
c [Å]	13.642(3)
α [°]	90
β [°]	103.249(4)
γ [°]	90
V [Å^3]	1387.5(6)
Z	6
λ [Å]	0.71073
ρ_{calc} [g·cm^{-3}]	1.839
θ [°]	2.189-30.936
μ [mm^{-1}]	0.162
F (000)	780
Reflections collected	13962
R_{int}	0.0549
Index ranges	−11 ≤ h ≤ 11 −18 ≤ k≤ 18 −19 ≤ l ≤ 19
Data/restraints/parameters	4362/0/268
Final R index ($I > 2\sigma(I)$)	R1 = 0.0561, wR2 = 0.1245
Final R index (all data)	R1 = 0.1202, wR2 = 0.1504
GOF	0.982
CCDC	1443112

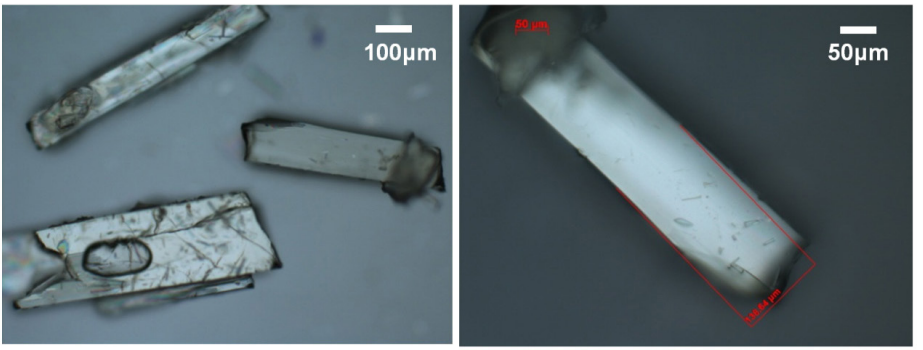

Figure 1. DABNT single-crystals

When the NH moieties are substituted with N−NH_2 groups, the intermolecular HB interactions become strengthened in the crystal packing. As shown in Figure 2, the N(4)−H(4A) ···O(4a) (–x+2, −y+2, −z) and N(4)−H(4A) ···N(14) (x+1/1, −y+3/2, z+1/2) interactions are strong and representative of HB interactions between two DABNT molecules. Both interactions show regular donor-H···acceptor (D−H···A) angles of 144(3)° and 142(3)°, respectively, and considerably short D−H···A distances of 2.43(3) Å and 2.63(3) Å, respectively. These HB interactions indicate that the increased numbers of amino groups enhances the structural stability of DABNT.

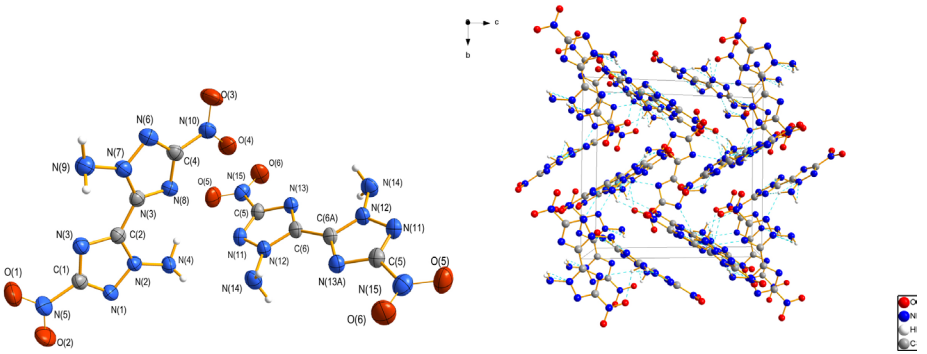

Figure 2. (a) Thermal ellipsoid plot (50%) and labelling scheme for DABNT. (b) Ball-and-stick packing diagram of DABNT viewed down the *a* axis. Dashed lines indicate the strong intermolecular hydrogen-bond interactions.

3.2 Non-isothermal decomposition properties

The investigation of the non-isothermal kinetic performance is increasingly important for the application and storage of newly-developed energetic materials [35]. According to the literature [28], DABNT immediately decomposes without a melting-point. The DSC and TG curves of DABNT at different temperatures are shown in Figures 3 and 4. It can be clearly seen that the decomposition peak of DABNT is 275.5 °C at a heating rate of 5 K·min^{-1}, which is higher than that of RDX (230 °C at the same heating rate). Additionally, DABNT possesses a main weight-loss of 89% before 500 °C at a heating rate of 5 K·min^{-1}.

To obtain the non-isothermal decomposition properties, such as apparent activation energy (E_a) and pre-exponential constant (A), after the exothermic decomposition reaction of DABNT, the methods of Kissinger, Ozawa, and Starink were employed as follows [36-38].

$$\ln\frac{\beta}{T_p^m} = -\frac{C_1 E_a}{RT_p} + C_2 \tag{1}$$

where, β is the heating rate (K·min^{-1}), T_p is the decomposition peak temperature (°C), E_a is the apparent activation energy (kJ·mol^{-1}), and C_1 and C_2 are constants taken from the references.

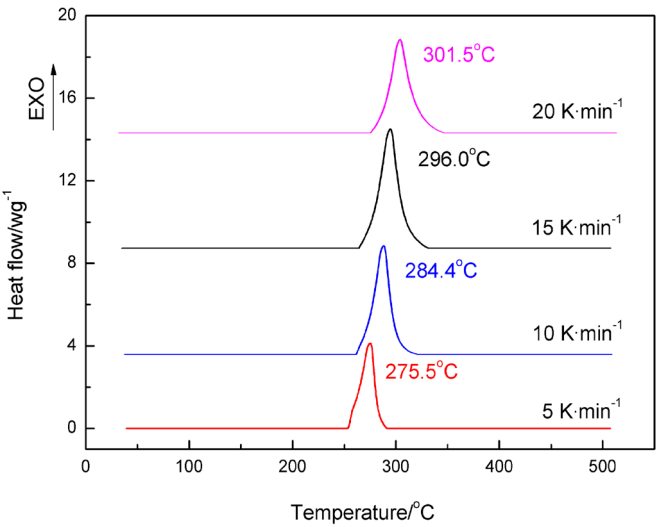

Figure 3. DSC curves measured at different heating rates, 5 K·min^{-1}, 10 K·min^{-1}, 15 K·min^{-1} and 20 K·min^{-1}

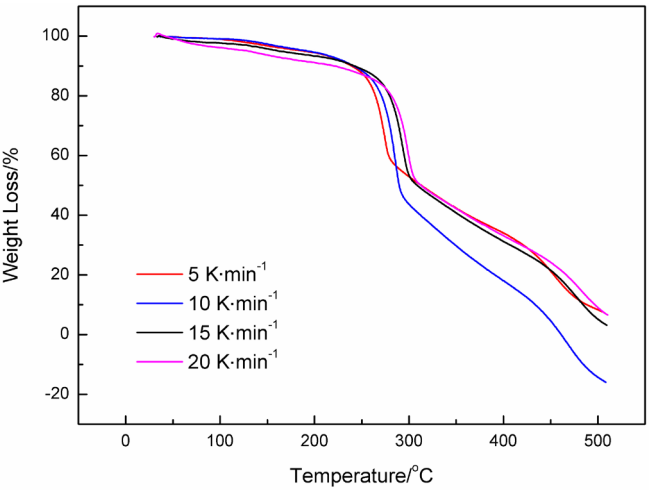

Figure 4. TG curves measured at different heating rates, 5 K·min^{-1}, 10 K·min^{-1}, 15 K·min^{-1} and 20 K·min^{-1}

Table 5. The chemical reaction kinetic parameters

Kinetic parameter	Kissinger's method	Ozawa's method	Starink's method
E [kJ·mol^{-1}]	122.9	123.2	123.5
ln(A) [s]	25.5	35.7	26.9
R	−0.95	−0.96	−0.95

The kinetic parameter values determined by the three methods and the linear correlation coefficients are listed in Table 5. It may be noted that the apparent activation energy (E_a) evaluated by the Kissinger, Ozawa and Starink methods agree well with each other, and the linear correlation coefficients are all close to 1, which suggests that the results are credible. In order, they were 122.9 kJ·mol^{-1}, 123.2 kJ·mol^{-1} and 123.5 kJ·mol^{-1}, respectively.

The entropy of activation ($\Delta S^{\neq}$), enthalpy of activation ($\Delta H^{\neq}$), and free energy of activation ($\Delta G^{\neq}$) of the decomposition reaction of DABNT corresponding to $T = T_{p0}$, $E_a = E_k$ and $A = A_K$ (adopted from Kissinger's method), were obtained by the Equations 2, 3 and 4, where k_B is the Boltzmann constant and h is the Planck constant. According to Equations 2, 3 and 4, they were −37.5 J·K^{-1}·mol^{-1}, 118.4 kJ·mol^{-1} and 138.7 kJ·mol^{-1}, respectively.

$$A = \frac{k_B T}{h} e^{\Delta S^{\neq} / R} \tag{2}$$

$$\Delta H^{\neq} = E - RT \tag{3}$$

$$\Delta G^{\neq} = \Delta H^{\neq} - T\Delta S^{\neq} \tag{4}$$

3.3 Thermolysis in a slowly heated IR cell

Thermolysis/RSFTIR was used to analyze the condensed phase products of the thermal decomposition of DABNT under a linear temperature increase in real time. The IR spectra of DABNT at different temperatures are shown in Figure 5. It is clearly observed that the absorption peaks of the amino groups disappear gradually after 270 °C, which means that most of the amino groups start to transform before the decomposition peak. As the temperature rose, most of the primary amine (−NH_2) vibrations between 3250 cm^{-1} and 3400 cm^{-1}, as well as vibrations between 3350 cm^{-1} and 3500 cm^{-1}, significantly decreased. Vibrations in the range of 3300 cm^{-1} and 3400 cm^{-1}, which apparently belong to the absorption peaks of secondary amines (−NH−), were detected as the temperature rose towards the decomposition peak. Meanwhile, it was found that the vibrations of the nitro groups vanished more slowly than those of the amine groups. It is evident that peaks in the characteristic spectral range of nitro groups, in the ranges of 800-920 cm^{-1}, 1300-1390 cm^{-1} and 1500-1600 cm^{-1}, were always visible, indicating that DABNT may merely lose one of the nitro groups at the first stage of thermal decomposition.

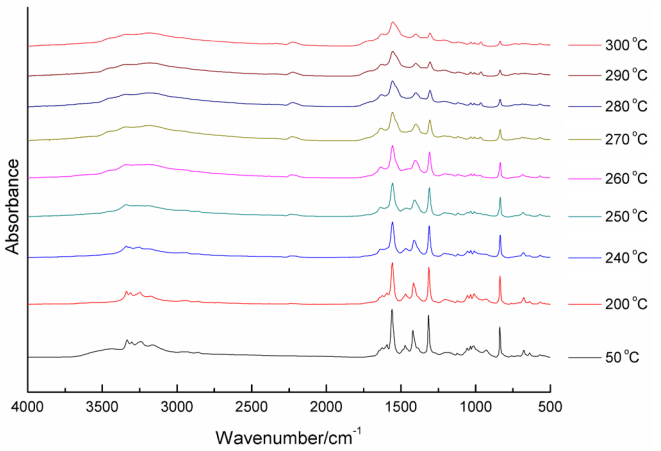

Figure 5. The selected peaks in the RSFT-IR spectra at different temperatures

3.4 Thermal decomposition gas product analysis

To study the decomposition mechanism, TG-IR was used to analyze the gaseous products during thermal decomposition. The temperature range was set in the range of 50-300 °C, since the sample did not decompose significantly before 275 °C at a heating rate of 5 °C·min^{-1}. The main gaseous products of DABNT are shown in Figure 6. The characteristic absorption peaks in the ranges 1000-1500 cm^{-1}, 2000-2350 cm^{-1} and near 2500 cm^{-1}, which belong to those of N_2O according to the database from the National Institute of Standards and Technology (NIST), can be clearly seen. With the increase in temperature, the absorption peaks of N_2O decrease slowly and the peaks of H_2O between 3500 cm^{-1} and 4000 cm^{-1} appear. At the end of decomposition, only a small amount of gas-phase products, such as N_2O and H_2O, are detected. Owing to the existence of numerous amino groups, another decomposition gaseous product is possibly N_2, but it cannot be detected by infrared.

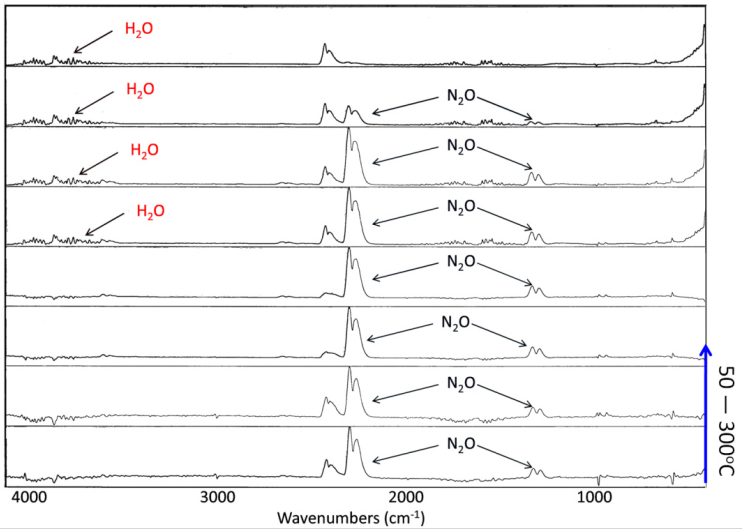

Figure 6. IR spectra of DABNT gaseous decomposition products with increase in temperature

3.5 Bond-dissociation energies

The bond-dissociation energy can reflect the change of the standard enthalpy while a chemical bond is cleaved by homolysis [39], which is helpful and frequently used in evaluating the thermal stability of energetic compounds in theoretical studies [40-43]. In the present case, to analyze the weakest bond in the thermal decomposition, DABNT was firstly optimized by the density functional

theory (DFT) method without imaginary frequencies and its geometrical structure is shown in Figure 7. The bond-dissociation energies (BDEs) of DABNT were then calculated at B3LYP/6-31+G** level by Gaussian 09 program [44] and are listed in Table 7. The BDE calculations show that the bond strength of N–NH_2 is stronger than that of C–NO_2. It can be seen that the BDEs of N5–NH_2 (332.22 kJ·mol^{-1}) and N9–NH_2 (332.20 kJ·mol^{-1}) are larger than those of C2–NO_2 and C6–NO_2 (282.85 kJ·mol^{-1}), suggesting that the C–NO_2 bond is thermally more unstable during the thermal decomposition stage than the N–NH_2 bond. This agrees with the results from TG-IR that N_2O was initially detected and H_2O was subsequently released with the increase in temperature.

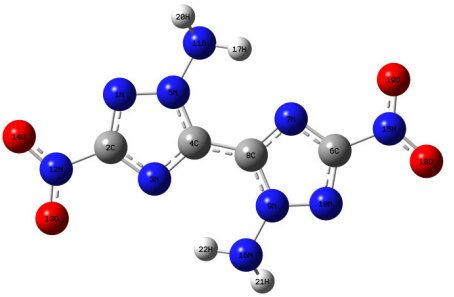

Figure 7. Optimized geometrical structure of DABNT with labelled atom numbers

Table 7. Bond-dissociation energies of the trigger bonds in DABNT

Bond type	C2–NO_2	C6–NO_2	N5–NH_2	N9–NH_2
BDE [kJ·mol^{-1}]	282.85	282.85	332.22	332.20

4 Conclusions

(1) We report a facile method for the synthesis of DABNT using the DBU salt of BNT and a dichloromethane solution of THA as the starting materials. Its structure was confirmed by optical spectroscopy, single-crystal XRD, NMR spectroscopy, elemental analysis and HRMS.

(2) The thermal decomposition behaviour was studied by DSC-TG. During the evaluation of non-isothermal thermodynamics, the apparent activation energy (E_a) determined by the Kissinger, Ozawa and Starink methods was 122.9 kJ·mol^{-1}, 123.2 kJ·mol^{-1} and 123.5 kJ·mol^{-1}, respectively. The entropy of activation ($\Delta S^{\neq}$), enthalpy of activation ($\Delta H^{\neq}$), and free energy of activation

($\Delta G^{\neq}$) of the decomposition reaction of DABNT were −37.5 $J \cdot K^{-1} \cdot mol^{-1}$, 118.4 $kJ \cdot mol^{-1}$ and 138.7 $kJ \cdot mol^{-1}$, respectively.

(3) The thermolysis mechanism was investigated by RSFTIR and TG-IR. Based on the absorption-peak evolution of the amino or nitro groups in the condensed framework in the RSFTIR analysis, DABNT may merely lose one nitro-group during the initial stage of thermal decomposition, with a structural transformation from primary amino group to secondary amino group. The TG-IR analysis reveals that the main gaseous decomposition products are N_2O and H_2O at the initial decomposition stage. In addition, BDE calculations show that the bond strength of $N-NH_2$ exceeds that of $C-NO_2$, which reveals that the $C-NO_2$ bond may break earlier than the $N-NH_2$ bond during the thermal decomposition.

Acknowledgment

We gratefully acknowledge financial support from the National Natural Science Foundation of China (11402237 and 11302200), Science and Technology Foundation of CAEP (2015B0302055), NSAF Foundation of National Natural Science Foundation of China and China Academy of Engineering Physics (No. U1530262).

References

[1] Klapötke, T. M. *Chemistry of High-Energy Materials*. 3rd ed., Berlin, Boston **2015**; ISBN 9783110439335.

[2] Gao, H.; Shreeve, J. M. Azole-based Energetic Salts. *Chem. Rev.* **2011**, *111*: 7377-7436.

[3] Bracuti, A. J. Crystal Structure of 4,5-Dinitroimidazole (45DNI). *J. Chem. Crystallogr.* **1998**, *28*: 367-371.

[4] Zaitsev, A. A.; Dalinger, I. L.; Shevelev, S. A. Dinitropyrazoles. *Russ. Chem. Rev.* **2009**, *78*: 589-627.

[5] Wang, J.; Dong, H.; Zhang, X.; Zhou, J. H.; Zhang, X. L.; Li, J. S. Synthesis, Thermal Stability and Sensitivity of 2,4-Dinitroimidazole. *Chin. J. Energ. Mater.* **2010**, *18*: 728-729.

[6] Janssen, J. W. A. M.; Habraken, C. L. Pyrazoles. VIII. Rearrangement of N-nitropyrazoles. The Formation of 3-Nitropyrazoles. *J. Org. Chem.* **1968**, *36*: 3081-3084.

[7] Hervé, G.; Roussel, C.; Graindorge, H. Selective Preparation of 3,4,5-Trinitro-1H-pyrazole: a Stable All-carbon-nitrated Arene. *Angew. Chem. Int. Ed.* **2010**, *49*: 3177-3181.

[8] Rahimi-Nasrabadi, M.; Zahedi, M. M.; Pourmortazavi, S. M.; Heydari, R.; Rai, H.; Jazayeri, J.; Javidan, A. Simultaneous Determination of Carbazole-based Explosives in Environmental Waters by Dispersive Liquid-liquid Microextraction Coupled to HPLC with UV-Vis Detection. *Microchim. Acta* **2012**, *177*: 145-152.
[9] Pourmortazavi, S. M.; Rahimi-Nasrabadi, M.; Rai, H.; Besharati-Seidani, A.; Javidan, A. Role of Metal Oxide Nanomaterials on Thermal Stability of 1,3,6-Trinitrocarbazole. *Propellants Explos. Pyrotech.* **2016**, *41*: 912-918.
[10] Dippold, A. A.; Klapötke, T. M. Nitrogen-rich Bis-1,2,4-triazoles – a Comparative Study of Structural and Energetic Properties. *Chem. Eur. J.* **2012**, *18*: 16742-16753.
[11] Dipplold, A. A.; Klapötke, T. M. A Study of Dinitro-bis-1,2,4-triazole-1,1'-diol and Derivatives: Design of High-performance Insensitive Energetic Materials by the Introduction of N-oxides. *J. Am. Chem. Soc.* **2013**, *135*: 9931-9938.
[12] Kettner, M. A.; Klapötke, T. M. New Energetic Polynitrotetrazoles. *Chem. Eur. J.* **2015**, *21*: 3755-3765.
[13] Gao, H.; Ye, C.; Gupta, O. D.; Xiao, J. C.; Hiskey, M. A.; Twamley, B.; Shreeve, J. M. 2,4,5-Trinitroimidazole-based Energetic Salts. *Chem. Eur. J.* **2007**, *13*: 3853-3860.
[14] Zhang, Y.; Guo, Y.; Joo, Y.; Parrish, D. A.; Shreeve, J. M. 3,4,5-Trinitropyrazole-based Energetic Salts. *Chem. Eur. J.* **2010**, *16*: 10778-10784.
[15] Chavez, D. E.; Parrish, D.; Preston, D. N.; Mares, I. W. Synthesis and Energetic Properties of 4,4',5,5'-Tetranitro-2,2'-biimidazolate (N4BIM) Salts. *Propellants Explos. Pyrotech.* **2012**, *37*: 647-652.
[16] Paraskos, A. J., Cooke, E. D., Caflin, K. C., Bishydrazinium and Diammonium Salts of 4,4',5,5'-Tetranitro-2,2'-biimidazole (TNBI): Synthesis and Properties. *Propellants Explos*. *Pyrotech.* **2015**, *40*: 46-49.
[17] Dippold, A. A.; Klapötke, T. M.; Martin, F. A.; Wiedbrauk, S. Nitraminoazoles Based on ANTA – a Comprehensive Study of Structural and Energetic Properties. *Eur. J. Inorg. Chem.* **2012**, *14*: 2429-2443.
[18] Song, J.; Wang, K.; Liang, L.; Bian, C.; Zhou, Z. High-energy-density Materials Based on 1-Nitramino-2,4-dinitroimidazole. *RSC Adv.* **2013**, *3*: 10859-10866.
[19] Zhang, Y.; Parrish, D. A.; Shreeve, J. M. 4-Nitramino-3,5-dinitropyrazole-based Energetic Salts. *Chem. Eur. J.* **2012**, *18*: 987-994.
[20] Yin, P.; Shreeve, J. M. From N-nitro to N-nitroamino: Preparation of High-performance Energetic Materials by Introducing Nitrogen-containing Ions. *Angew. Chem. Int. Ed.* **2015**, *54*: 14513-14517.
[21] Yin, P.; Parrish, D. A.; Shreeve, J. M. Energetic Multifunctionalized Nitraminopyrazoles and Their Ionic Derivatives: Ternary Hydrogen-bond Induced High Energy Density Materials. *J. Am. Chem. Soc.* **2015**, *137*: 4778-4786.
[22] Duddu, R.; Dave, P. R.; Damavarapu, R.; Gelber, N.; Parrish, D. Synthesis of N-amino- and N-nitramino-nitroimidazoles. *Tetrahedron Lett.* **2010**, *51*: 399-401.
[23] Breiner, M. M.; Chavez, D. E.; Parrish, D. A. Nucleophilic Reactions of the Bis Ammonium Salt of 4,4',5,5'-Tetranitro-2,2'-biimidazole. *Synlett* **2013**, *24*: 519-521.
[24] Jing, M.; Shu, Y.; Wang, J.; Ma, Q.; Zhang, X.; Huang, Y. Synthesis, Crystal

Structure and Thermal Property of 1-Amino-2,4-dinitroimidazole. *Chin. J. Energ. Mater.* **2014**, *22*: 454-457.

[25] Jiang, T.; Zhang, X.; Jing, M.; Shu, Y.; Wang, J. Synthesis, Crystal Structure and Thermal Property of 1-Amino-3,5-dinitropyrazole. *Chin. J. Energ. Mater.* **2014**, *22*: 654-657.

[26] Yin, P.; Zhang, J.; He, C.; Parrish, D. A.; Shreeve, J. M. Polynitro-substituted Pyrazoles and Triazoles as Potential Energetic Materials and Oxidizers. *J. Mater. Chem. A* **2014**, *3*: 3200-3208.

[27] Chavez, D. E.; Bottaro, J. C.; Petrie, M.; Parrish, D. A. Synthesis and Thermal Behavior of a Fused, Tricyclic 1,2,3,4-Tetrazine Ring System. *Angew. Chem. Int. Ed.* **2015**, *54*: 12973-12975.

[28] Yin, P.; Shreeve, J. M. From N-nitro to N-nitroamino: Preparation of High-performance Energetic Materials by Introducing Nitrogen-containing Ions. *Angew. Chem. Int. Ed.* **2015**, *54*: 14513-14517.

[29] Szala, M.; Lewczuk, R. New Synthetic Methods for 4,4',5,5'-Tetranitro-2,2'-bi-1H-imidazole (TNBI). *Cent. Eur. J. Energ. Mater.* **2015**, *12*: 261-270.

[30] Shamsipur, M.; Pourmortazavi, S. M.; Hajimirsadeghi, S. S.; Atifeh, S. M. *Fuel* **2012**, *95*: 394-399.

[31] Tamura, Y.; Minamikawa, J.; Sumoto, K.; Fujii, S.; Ikeda, M. Synthesis and Some Properties of *O*-acyl- and *O*-nitrophenylhydroxylamines. *J. Org. Chem.* **1973**, *38*: 1239-1241.

[32] Ma, Q.; Wang, J.; Zhang, X.; Shu, Y. Synthesis and Performance of 2,4,6-Trimethylbenzenesulfonic Hydroxylamine. *Chin. J. Energ. Mater.* **2013**, *21*: 133-134.

[33] Sheldrick, G. M. *SHELXS 97*, University of Göttingen, Germany **1990**.

[34] Sheldrick, G. M. *SHELXL 97*, University of Göttingen, Germany **1997**.

[35] Liu, Y.; Jiang, Y. T.; Zhang, T. L.; Feng, C. G.; Yang, L. Thermal Kinetic Performance and Storage Life Analysis of a Series of High-Energy and Green Energetic Materials. *J. Therm. Anal. Calorim.* **2015**, *119*: 659-670.

[36] Kissinger, H. E. Reaction Kinetics in Differential Thermal Analysis. *Anal. Chem.* **1957**, *29*: 1702-1706.

[37] Ozawa, T. A New Method of Analyzing Thermogravimetric Data. *B. Chem. Soc. Jap.* **1957**, *38*: 1881-1886.

[38] Boswell, P. G. Calculation of Activation Energies Using a Modified Kissinger Method. *J. Therm. Anal. Calorim.* **1980**, *18*: 353-356.

[39] McNaught, A. D., Wilkinson, A. *Compendium of Chemical Terminology*. 2nd ed., Cambridge, UK **1997**; ISBN 0865426848.

[40] Yan, Q.; Zeman, S. Theoretical Evaluation of Sensitivity and Thermal Stability for High Explosives Based on Quantum Chemistry Methods: a Brief Review. *Int. J. Quant. Chem.* **2013**, *113*: 1-14.

[41] Jing, S.; Liu, Y.; Liu, D.; Guo, J. Synthesis and Theoretical Studies of a New High Explosive, N,N,-Bis(3-aminofurazan-4-yl)-4,4'-diamino-2,2',3,3',5,5',6,6'-octanitroazobenzene. *Cent. Eur. J. Energ. Mater.* **2015**, *12*: 745-755.

[42] Ma, Q.; Jiang, T.; Zhang, X.; Fan, G.; Wang, J.; Huang, J. Theoretical Investigations on 4,4',5,5'-Tetranitro-2,2'-1H,1'H-2,2'-biimidazole Derivatives as Potential Nitrogen-rich High Energy Materials. *J. Phys. Org. Chem.* **2015**, *28*: 31-39.

[43] Ma, Q.; Liao, L. Y.; Cheng, B. B.; Fan, G. J.; Huang, J. L.; Wang, J. Construction of New Insensitive Explosives: Fused N_5-Chain N^1,N^3,N^5-(1,2,3,4-tetrazole-5-nitro)-1,3,5-triamino-2,4,6-trinitrobenzene Derivatives. *Polycyc. Aromat. Comp.* **2016**, *36*: 639-655.

[44] Frisch, M. J.; Trucks, G. W.; Schlegel, H. B.; Scuseria, G. E.; Robb, M. A.; Cheeseman, J. R.; Scalmani, G.; Barone, V.; Mennucci, B.; Petersson, G. A.; Nakatsuji, H.; Caricato, M.; Li, X.; Hratchian, H. P.; Izmaylov, A. F.; Bloino, J.; Zheng, G.; Sonnenberg, J. L.; Hada, M.; Ehara, M.; Toyota, K.; Fukuda, R.; Hasegawa, J.; Ishida, M.; Nakajima, T.; Honda, Y.; Kitao, O.; Nakai, H.; Vreven, T.; Montgomery, Jr J. A.; Peralta, J. E.; Ogliaro, F.; Bearpark, M.; Heyd, J. J.; Brothers, E.; Kudin, K. N.; Staroverov, V. N.; Keith, T.; Kobayashi, R.; Normand, J.; Raghavachari, K.; Rendell, A.; Burant, J. C.; Iyengar, S. S.; Tomasi, J.; Cossi, M.; Rega, N.; Millam, J. M.; Klene, M.; Knox, J. E.; Cross, J. B.; Bakken, V.; Adamo, C.; Jaramillo, J.; Gomperts, R.; Stratmann, R. E.; Yazyev, O.; Austin, A. J.; Cammi, R.; Pomelli, C.; Ochterski, J. W.; Martin, R. L.; Morokuma, K.; Zakrzewski, V. G.; Voth G. A.;, Salvador, P.; Dannenberg, J. J.; Dapprich, S.; Daniels, A. D.; Farkas, O.; Foresman, J. B.; Ortiz, J. V.; Cioslowski, J., Fox, D. J. *GAUSSIAN 09 (Revision D.01)*: Gaussian, Inc, **2009**.